Inorganic Chemistry

Article

pubs.acs.org/IC

Soluble Molybdenum(V) Imido Phthalocyanines and Pyrazinoporphyrazines: Crystal Structure, UV−vis and Electron Paramagnetic Resonance Spectroscopic Studies

Elisabeth Seikel, Benjamin Oelkers, Olaf Burghaus, and Jörg Sundermeyer*

Material Sciences Center and Fachbereich Chemie, Philipps-Universität Marburg, Hans-Meerwein-Straße, 35032 Marburg, Germany

Supporting Information

ABSTRACT: Soluble alkyl and aryl imido phthalocyanines [Pc#Mo(NR)Cl] (R = *t*Bu, Mes) with molybdenum(V) as central metal were prepared and studied by UV−vis and electron paramagnetic resonance (EPR) spectroscopy. As structural analogue to the weakly aggregating, soluble alkyl substituted Pc# ligand, a new, more electron deficient octaazaphthalocyanine, the pyrazinoporphyrazine ligand Ppz#, was designed. The respective alkyl and aryl imido complexes [Ppz#Mo(NR)Cl] are the first examples of molybdenum pyrazinoporphyrazines. UV−vis and EPR spectra revealed unexpected differences between the alkyl and the aryl imido complexes, indicating different electronic structures depending on the nature of the axial ligand. The octahedral coordination of the molybdenum atoms by the axial NR and Cl ligands and the equatorial macrocycles could be verified by EPR spectroscopy. This result was also confirmed by the crystal structure of [Pc#Mo(NMes)Cl], which crystallizes from CH_2Cl_2 in the cubic space group $Im\bar{3}$.

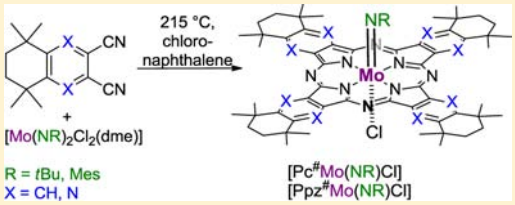

INTRODUCTION

Phthalocyanines and their metal complexes are one of the most important and versatile classes of organic chromophores produced in industry.[1] While 90% of the phthalocyanine production resembles valuable applications as pigments for inks, paints, and thermoplastics, a growing and even more valuable fraction resembles high-tech applications in optoelectronic devices.[2−5] Among these applications, organic field effect transistors (OFETs),[6] dye sensitized solar cells (DSSCs),[7−13] and nonlinear optical materials (NLO)[14] are of particular interest to date. Phthalocyanine complexes can be readily obtained by reductive cyclotetramerization of phthalonitrile in the presence of an appropriate metal precursor at high temperatures. The introduction of bulky substituents at the Pc periphery increases the solubility of the complexes (Figure 1). While much research has been dedicated to the effect of peripheral substituents on [PcM], significantly less is known about the effects of axial substituents at the metal center. This is mainly due to the insolubility of unsubstituted phthalocyanines which hampers their selective functionalization. We are interested both in the axial functionalization of practically insoluble Pc complexes as well as soluble, alkyl substituted analogues.[15−21] We decided to restrain our studies of soluble complexes to the methyl substituted Pc# ligand first described by Mikhalenko et al.[22] because of its symmetry and the absence of functional groups in the ligand periphery (Figure 1).

Molybdenum phthalocyanines are interesting materials because of the different possible oxidation states of the central metal. Mo^{IV} and Mo^{V} phthalocyanines have therefore been employed in redox reactions[23,24] such as O_2 reduction[25] or D-glucose oxidation.[26] In all these reactions, molybdenum oxido phthalocyanines were employed. Besides oxido complexes,[27] halogenido[28] and nitrido[19,29] complexes are also known as well as dimeric compounds.[30] In our research group, a synthetic protocol for organoimido chlorido complexes [PcMo(NR)Cl] was developed for the unsubstituted Pc ligand.[17] We wanted to expand these studies to soluble, alkyl substituted Pc# complexes and investigate the spectroscopic properties of the paramagnetic d^1 molybdenum compounds in detail.

Because of their similar structural features, preparation and properties, metal pyrazinoporphyrazines (Ppz) and phthalocyanines are usually investigated with regard to similar optoelectronic applications.[5] The absorption maximum of pyrazinoporphyrazines is shifted hypsochromically compared to analogous phthalocyanines because of the more electron deficient macrocyclic ligand and a larger gap between the highest occupied molecular orbital (HOMO) and the lowest unoccupied molecular orbital (LUMO).[31] The synthesis of soluble, chemically and thermally robust, and isomerically pure derivatives of such azaphthalocyanines is of current interest.[32] We decided to develop the new alkyl substituted Ppz# ligand which is the structural analogue to Pc# (Figure 1).[33]

This work is focused on the synthesis of molybdenum Ppz# complexes, which is of particular interest as no examples for molybdenum pyrazinoporphyrazines have been described in the literature. Given the optoelectronic features of Ppz compounds and the potential application of macrocycle-supported molybdenum complexes in redox reactions, PpzMo compounds with molybdenum in different oxidation states are interesting target compounds.

Received: December 7, 2012
Published: March 28, 2013

dx.doi.org/10.1021/ic3026914 | *Inorg. Chem.* 2013, 52, 4451−4457

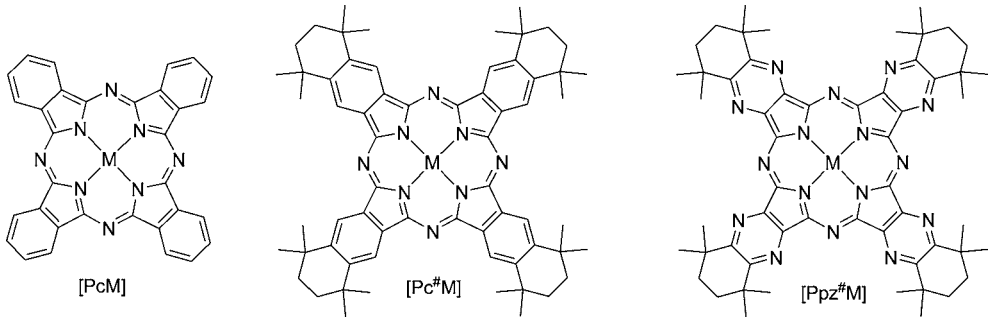

Figure 1. Structures of metal phthalocyanines [PcM] and [Pc#M] as well as pyrazinoporphyrazine [Ppz#M].

EXPERIMENTAL SECTION

General Procedures. 3,3,6,6-Tetramethylcyclohexane-1,2-dione **1**,[34,35] $[Mo(NtBu)_2Cl_2(dme)]$[36] and $[Mo(NMes)Cl_2(dme)]$[37] were prepared according to literature procedures. 6,7-Dicyano-1,1,4,4-tetramethyltetraline **2** was prepared as described by Mikhalenko et al.[22] and purified by column chromatography (silica gel, CH_2Cl_2) prior to use. Chloronaphthalene was obtained from Acros as a mixture of 1-chloronaphthalene (90%) and 2-chloronaphthalene (10%). Solvents were dried according to standard methods and stored under inert gas over molecular sieves.

^1H and ^{13}C NMR spectra were recorded on a Bruker Avance 300. Elemental analyses of C, H, N, and S were carried out using an Elementar vario MICRO cube.

X-band electron paramagnetic resonance (EPR) spectra were recorded on a Bruker ESP 300 spectrometer. Solutions of the substances (c = 1 mM) in quartz tubes (d = 4 mm) were used. For Q-band spectra, a modified Varian E15 spectrometer and solutions (c = 2 mM) in quartz tubes (d = 2 mm) were used. Data analyses were carried out with a locally developed fit/simulation program (nsimepr2). The usual Hamiltonian, (see for instance[38,39]), is used in second order approximation for the ^{95,97}Mo hyperfine (hf) interactions and in first order for the superhyperfine (shf) lines of ^{14}N and ^{35,37}Cl. Isotropic fits account for the m_I dependent line width effect. Hf tensors axes are allowed to have independent orientation with respect to the g-tensor axes. Deviations from colinearity were small (<3°), hence all Euler angles were set to zero for all fits. To enhance reliability and accuracy of the fit results, the anisotropic X- and Q-band spectra of each substance were simultaneously fitted with an identical set of parameters, but allowing the line width and intensity to adjust independently.

IR spectra were recorded on a Bruker Alpha FT-IR spectrometer with an ATR measurement setup (diamond cell) in a glovebox using neat samples. UV−vis spectra were recorded on an Avantes AvaSpec-2048 spectrometer in a glovebox. ESI and APCI mass spectra were taken on a Finnigan LTQ-FT spectrometer using dichloromethane as solvent.

XRD analyses were performed on a Stoe IPDS 2 area detector system using Mo K_α radiation (λ = 71.073 pm) at 100 K. Stoe IPDS software[40] was used for integration and data reduction, structure solution and refinement was done with the WinGX program[41] suite using SIR2004[42] and SHELX-97.[43] Molecular graphics were produced with Diamond 3.2g.[44] The disordered solvent (dichloromethane) could not be modeled completely and was thus in part removed using PLATON/SQUEEZE.

5,5,8,8-Tetramethyl-5,6,7,8-tetrahydroquinoxaline-2,3-carbodinitrile 3. A 5.00 g portion of 3,3,6,6-tetramethylcyclohexane-1,2-dione **1** (29.7 mmol, 1.0 equiv), 3.86 g of 2,3-diaminomaleonitrile (35.7 mmol, 1.2 equiv), and a catalytic amount of *p*TsOH were refluxed in 85 mL of dry ethanol for 3.5 h. The reaction progress was monitored via TLC (CH_2Cl_2). After cooling, the solvent was removed under reduced pressure. The crude product was taken up in CH_2Cl_2 and extracted with water. The organic layer was dried over $MgSO_4$ and evaporated. The brown product was purified by column chromatography (CH_2Cl_2), yielding 5.51 g of **3** (22.9 mmol, 77%) as a colorless solid. ^1H NMR (300 MHz, $CDCl_3$): δ = 1.83 (s, 4H, CH_2), 1.34 (s, 12H, CH_3) ppm. ^{13}C NMR (75 MHz, $CDCl_3$): δ = 164.0, 130.2, 113.4, 38.5, 33.0, 29.5 ppm. IR: υ = 2969 (s), 2939 (s), 2869 (m), 2232 (w, $\nu_{C\equiv N}$), 1517 (m), 1458 (s), 1361 (m), 1346 (s), 1301 (s), 1260 (m), 1188 (m), 1126 (s), 1022 (s), 955 (m), 799 (s), 720 (m). MS (ESI-HR(+)): m/z = 241.1440 $[M+H]^+$, $C_{14}H_{17}N_4$ requires: 241.1448.

$Ppz^{\#}H_2$ 3a. A 146 mg portion of lithium (20.8 mmol, 5.0 equiv) was completely converted to LiOOct by adding 10 mL of 1-octanol. One gram of **1** (4.17 mmol, 1.0 equiv) was added, and the mixture was heated to 130 °C overnight. The mixture turned blue and violet microcrystals precipitated. After cooling, 60 mL of methanol and 1 mL of H_3PO_4 (80%) were added to obtain the protonated ligand. The blue solid was collected and washed three times with methanol, hexane, and dried under vacuum. Yield: 240 mg (0.25 mmol, 24%). ^1H NMR (300 MHz, $CDCl_3$): δ = 2.22 (s, 16H), 1.93 (s, 48H), −1.06 (s, 2H, N*H*). IR: υ = 3282 (w), 2959 (m), 2920 (m), 2859 (m), 1543 (w), 1456 (m), 1329 (m), 1254 (s), 1236 (s), 1141 (s), 1086 (s), 805 (m), 686 (s). UV−vis (CH_2Cl_2): λ = 655 (s), 621 (s), 606 (sh), 576 (sh), 342 (s). MS (APCI-HR(+)): m/z = 963.5732 $[M+H]^+$, $C_{56}H_{67}N_{16}$ requires 963.5729.

General Procedure for the Preparation of Compounds 4−7. Four equivalents of the respective dinitrile and 1.0 equiv of $[Mo(NR)_2Cl_2(dme)]$ (R = *t*Bu, Mes) in chloronaphthalene (ca. 1 mL per 200 mg dinitrile) were placed in a bath of wood's metal preheated to 215 °C and stirred for 1 h. After cooling, the product was precipitated by addition of hexane and collected by filtration. The solid material was extracted with acetonitrile and diethyl ether and dried under vacuum.

[$Pc^{\#}$Mo(N*t*Bu)Cl] 4. 200 mg of **2** (0.84 mmol, 4.0 equiv), 72 mg of $[Mo(NtBu)_2Cl_2(dme)]$ (0.21 mmol, 1.0 equiv), 1 mL of chloronaphthalene. Yield: 53 mg green solid (0.05 mmol, 22%). EPR (9.2 GHz, chloronaphthalene/toluene 1:3, 60 K): g_{iso} = 1.9810. IR: υ = 2955 (m), 2922 (m), 2859 (m), 1616 (w), 1470 (m), 1317 (s), 1187 (m), 1072 (s), 983 (w), 897 (m), 745 (m), 543 (w). UV−vis (CH_2Cl_2): λ = 738 (s), 665 (sh), 373 (s). MS (APCI-HR(+)): m/z = 1121.5680 $[M-Cl]^+$, $C_{68}H_{81}MoN_9$ requires: 1121.5682.

[$Pc^{\#}$Mo(NMes)Cl] 5. 1.65 g of **2** (6.93 mmol, 4.0 equiv), 844 mg of $[Mo(NMes)_2Cl_2(dme)]$ (1.73 mmol, 1.0 equiv), 8.5 mL of chloronaphthalene. Yield: 730 mg brown solid (0.60 mmol, 35%). Suitable single crystals for X-ray diffraction were obtained from a saturated CH_2Cl_2 solution at 4 °C. EPR (9.2 GHz, chloronaphthalene/toluene 1:3, 40 K): g_{iso} = 1.9782. IR: υ = 2955 (m), 2923 (m), 2858 (m), 1603 (w), 1458 (m), 1318 (s), 1187 (m), 1072 (s), 984 (m), 876 (m), 761 (w), 706 (w), 543 (w). UV−vis (CH_2Cl_2): λ = 756 (s), 680 (sh), 382 (s), 282 (m). MS (APCI-HR(+)): m/z = 1183.5822 $[M-Cl]^+$, $C_{73}H_{83}MoN_9$ requires: 1183.5840.

[$Ppz^{\#}$Mo(N*t*Bu)Cl] 6. 200 mg of **3** (0.83 mmol, 4.0 equiv), 83 mg of $[Mo(NtBu)_2Cl_2(dme)]$ (0.21 mmol, 1.0 equiv), 1 mL of chloronaphthalene. Yield: 62 mg green solid (0.05 mmol, 26%). EPR (9.2 GHz, chloronaphthalene/toluene 1:3, 40 K): g_{iso} = 1.9808. IR: υ = 2954 (m), 2926 (m), 2865 (m), 1549 (w), 1455 (m), 1331 (m), 1258 (vs), 1187 (m), 1074 (s), 1000 (m), 882 (s), 697 (s), 433 (m). UV−vis (CH_2Cl_2): λ = 662 (s), 610 (sh), 367 (s), 308 (m), 269 (w). MS (APCI-HR(+)): m/z = 1165.5029 $[M+H^+]$, $C_{60}H_{73}ClMoN_{17}$

dx.doi.org/10.1021/ic3026914 | Inorg. Chem. 2013, 52, 4451−4457

requires: 1165.5059; m/z = 1130.5352 $[M\text{-}Cl+H]^+$, $C_{60}H_{74}MoN_{17}$ requires: 1130.5377.

[Ppz#Mo(NMes)Cl] 7. 500 mg of **3** (2.08 mmol, 4.0 equiv), 230 mg of $[Mo(NMes)_2Cl_2(dme)]$ (0.47 mmol, 1.0 equiv), 1 mL of chloronaphthalene. Yield: 112 mg of green solid (0.09 mmol, 19%). EPR (9.2 GHz, chloronaphthalene/toluene 1:3, 40 K): g_{iso} = 1.9790. IR: υ = 2954 (m), 2925 (m), 2860 (m), 1601 (w), 1546 (w), 1455 (m), 1330 (m), 1257 (vs), 1186 (m), 1070 (m), 1000 (s), 881 (s), 696 (s), 492 (m), 432 (m). UV–vis (CH_2Cl_2): λ = 672 (s), 640 (sh), 371 (s), 307 (m), 272 (w). MS (APCI-HR(+)): m/z = 1227.5226 $[M+H^+]$, $C_{65}H_{75}ClMoN_{17}$ requires: 1227.5217; m/z = 1191.5460 $[M\text{-}Cl+H]^+$, $C_{65}H_{75}MoN_{17}$ requires: 1191.5457.

DISCUSSION

Synthesis. Analogously to the cyclotetramerization of phthalonitriles to phthalocyanines, pyrazinoporphyrazines can be prepared starting from the respective pyrazine dinitrile. Hence, to prepare Ppz# complexes, the structural analogues to Pc# complexes, we had to develop a synthesis for **3** (Figure 2). Like the corresponding phthalonitrile **2**, **3** bears an anellated tetramethyl cyclohexenyl group.

2 3

Figure 2. Structures of dinitriles **2** and **3**.

Following a standard synthetic protocol for the preparation of pyrazine dinitriles, **3** could be prepared by a condensation of diaminomaleonitrile (DAMN) and diketone **1**[34,35] in ethanol (Scheme 1). After purification by column chromatography, **3** was obtained as a colorless solid in 77% yield. **3** can easily be converted into the free ligand $Ppz^{\#}H_2$ by reaction with lithium octanolate in 1-octanol at 130 °C.

Scheme 1. Preparation of 3 and 3a

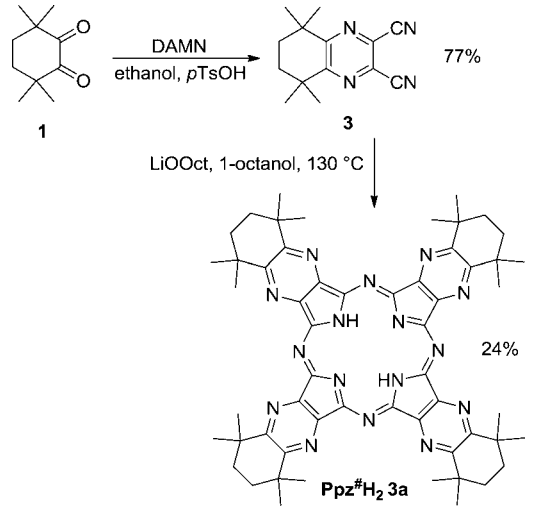

The unsubstituted phthalocyanine compounds [PcMo(N*t*Bu)Cl] and [PcMo(NMes)Cl] can be prepared from phthalonitrile and the respective molybdenum imido complexes $[Mo(NR)_2Cl_2(dme)]$ (R = *t*Bu, Mes) at 220 °C without the use of a solvent.[17] An analogous neat reaction of the substituted dinitrile **2** produced only traces of the desired product. However, $[Pc^{\#}Mo(NR)Cl]$ (**4**, **5**) and $[Ppz^{\#}Mo(NR)Cl]$ (**6**, **7**) (R = *t*Bu, Mes) could be prepared successfully by carrying out the reaction in chloronaphthalene (Scheme 2). The

Scheme 2. Synthesis of Compounds 4–7

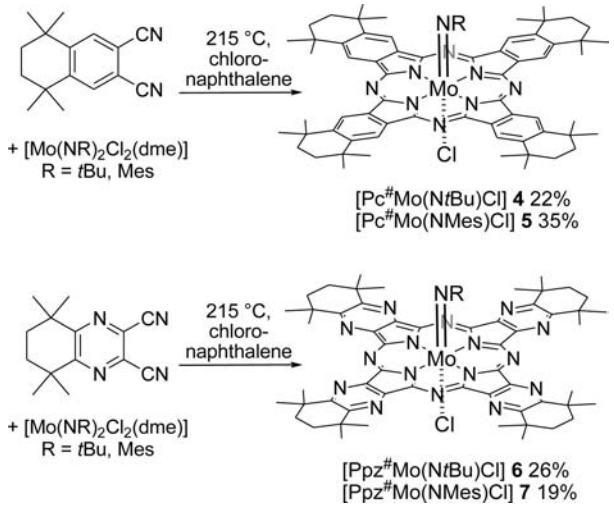

macrocyclic products were obtained as intensely green or brown solids in 19–35% yield. The products are formed as a consequence of a complex redox reaction cascade at a Lewis acidic imido metal template, in which an imido group $[NR]^{2-}$ is formally lost as nitrene [NR] diradical and a coordinated chlorido ligand as chlorine radical. The result of this multistep reaction of phthalo- and pyrazinodinitrile is the formal substitution of an imido ligand $[NR]^{2-}$ by a symmetrical and soluble 42π Hückel aromatic $[Pc^{\#}]^{2-}$ or $[Ppz^{\#}]^{2-}$ ligand.

UV–vis Spectroscopy. The UV–vis spectra of phthalocyanines $[Pc^{\#}Mo(NtBu)Cl]$ **4** and $[Pc^{\#}Mo(NMes)Cl]$ **5** as well as their pyrazinoporphyrazine analogues $[Ppz^{\#}Mo(NtBu)Cl]$ **6** and $[Ppz^{\#}Mo(NMes)Cl]$ **7** in CH_2Cl_2 are shown in Figure 3.

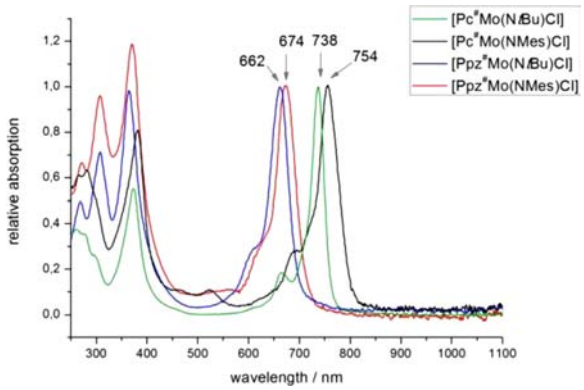

Figure 3. UV–vis spectra of compounds **4**–**7** in CH_2Cl_2.

The Q-band absorption maxima of the phthalocyanine compounds lie in the NIR region (738 and 756 nm). This explains why $[Pc^{\#}Mo(NMes)Cl]$ appears brown. As expected, the Q-band absorptions of the electron deficient pyrazinoporphyrazines are shifted 76 and 80 nm hypsochromically to 662 and 672 nm, respectively. The large differences between the absorption maxima of the *t*Bu-substituted complexes and their mesityl analogues are somewhat surprising. Usually, the exchange of an axial alkyl substituent for an aryl substituent

dx.doi.org/10.1021/ic3026914 | Inorg. Chem. 2013, 52, 4451–4457

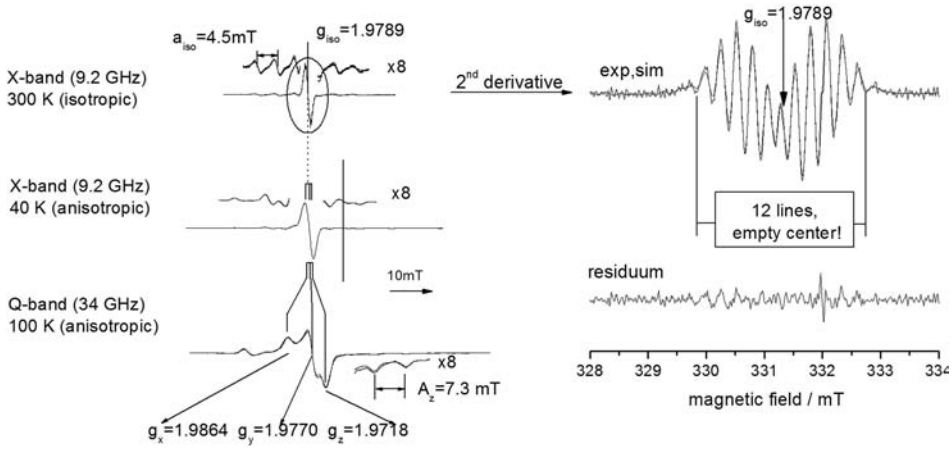

Figure 4. Q- and X-band spectra of **5**. For details, see discussion.

does not affect the electronic spectra of metal phthalocyanines.[18,21] This is in accord with the Q-band in Pc or Ppz complexes being derived from the HOMO−LUMO ($\pi-\pi^*$) transition of the aromatic system.[45] These orbitals are located on the planar ligand and are usually not much affected by an exchange of axial ligands. To better understand the electronic structures of the novel complexes, we recorded EPR spectra of the paramagnetic Mo^V phthalocyanines and pyrazinoporphyrazines.

EPR Spectroscopy. Q- and X-band EPR spectra of the paramagnetic molybdenum complexes were measured in chloronaphthalene/toluene (1:3) at various temperatures. Q- and X-band EPR spectra and fit results of **5** are depicted in Figure 4. The isotropic X-band spectrum and computer fit reveal a g_{iso} value of 1.9789 confirming the d^1 electronic structure of the novel compound. The isotropic hf constant of the ^{95,97}Mo isotopes (both $I = 5/2$), a_{iso} = 4.5 mT, and the isotropic g value compare well to those of [PcMo(N*t*Bu)Cl] (g_{iso} = 1.984, a_{iso} = 4.6 mT),[17] and other macrocycle-supported Mo^V complexes.[17,29,46,47]

The central line of the isotropic spectrum (Figure 4, at top right, second derivative), which is unaffected by hf interactions of magnetic molybdenum isotopes (74.5%), shows 12 well resolved equally spaced shf lines with an empty center. This is a clear indication that 4 equal ^{14}N ($I = 1$) shf couplings (9 lines) are further split by one ^{35,37}Cl atom ($I = 3/2$) with similar hf coupling, resulting in 12 separated lines. The fit confirms these assumptions and disproves a model with 5 ^{14}N hf couplings (11 lines, central line). An assumed fifth nitrogen hf coupling must be smaller than the visible line width of 0.3 mT. Comparable superhyperfine fit parameters were obtained for the room temperature X-band spectrum for the second mesityl imido complex **7** (not displayed). High resolution isotropic data for **4** and **6** are not available, but we expect a significant alteration of the superhyperfine pattern because of the clear differences of the Mo−Cl bond distances between N*t*Bu and NMes complexes (see discussion of crystal structure below), which will certainly change the spin density at the axial Cl atoms and therefore will change the superhyperfine couplings, too. A quantitative comparison of superhyperfine couplings should not be made unless being supported by theoretical calculations, though.

Frozen solutions of **5** were measured in X- (Figure 4, left middle) and Q-band (Figure 4, bottom left). At X-band the Zeeman interaction is small compared to the anisotropic hf splitting. The central line shows only a small deviation from an isotropic Gaussian line shape. At Q-band a rhombic g-anisotropy with three resolved g-tensor components is visible.

In Figure 5 X-band (left) and Q-band (right) spectra of frozen solutions of **4**−**7** are shown. The most striking features

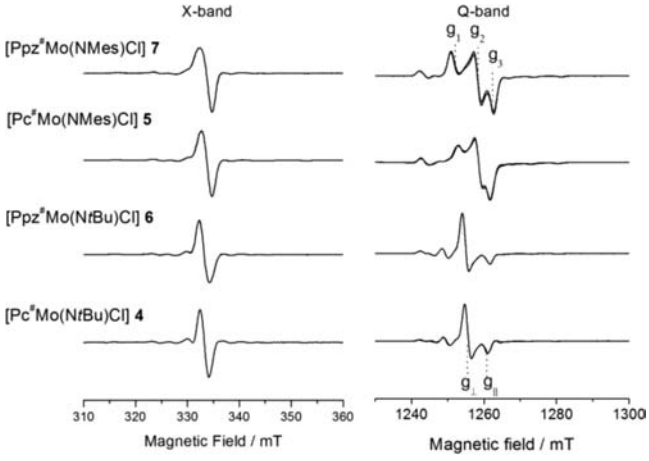

Figure 5. Frozen solution spectra in X-band (left) and Q-band (right). Bottom: spectra of C_{4v}-symmetric complexes [Pc#Mo(N*t*Bu)Cl] **4** and [Ppz#Mo(N*t*Bu)Cl] **6**, top: spectra of C_{2v}-symmetric complexes [Pc#Mo(NMes)Cl] **5** and [Ppz#Mo(NMes)Cl] **7**.

of the spectra, nicely resolved at Q-band, are the differences between the alkyl imido complexes **4** and **6** and their aryl imido analogues **5** and **7**. In the case of the N*t*Bu-substituted complexes, axial symmetric spectra ($g_\perp > g_\parallel$) are observed, while rhombic spectra are observed in the case of the NMes-substituted complexes.

The results of the EPR spectroscopy of complexes **4**−**7** are summarized in Table 1. The most striking result is that the alkyl imido complexes **4** and **6** are C_{4v}-symmetric, which is confirmed by the anisotropic g-values $g_\perp$ and $g_\parallel$. In contrast to this, the symmetry is lowered to C_{2v} in the case of aryl imido analogues **5** and **7**. The different symmetries of the complexes depending on the nature of the axial imido ligand are in accord with the unexpected differences between the UV−vis spectra of the N*t*Bu and NMes compounds.

The symmetry lowering associated with the exchange of an axial alkyl imido group for an aryl imido group requires the lifting of the degeneracy of the d_{xz} and d_{yz} orbitals in the C_{2v}-

dx.doi.org/10.1021/ic3026914 | Inorg. Chem. 2013, 52, 4451−4457

Table 1. Isotropic and Anisotropic EPR Parameters of Compounds 4−7[a]

	[Pc#Mo(NtBu)Cl] **4**	[Pc#Mo(NMes)Cl] **5**	[Ppz#Mo(NtBu)Cl] **6**	[Ppz#Mo(NMes)Cl] **7**
g_x	1.9830[b]	1.9864	1.9838	1.9892
g_y	1.9846[b]	1.9770	1.9838	1.9782
g_z	1.9744	1.9718	1.9724	1.9713
1/3 ⟨g⟩	1.9806	1.9786	1.9800	1.9796
g_{iso}	1.9810	1.9789	1.9801	1.9796
A_x/mT	3.2	3.22	3.41	3.22
A_y/mT	3.4	3.30	3.31	3.43
A_z/mT	7.3	7.34	7.46	7.27
1/3 ⟨A⟩/mT	4.6	4.62	4.72	4.64
ΔB_x/mT	1.5 (+1.2)	1.76 (+1.16)	1.85 (−0.01)	1.62 (+0.53)
ΔB_y/mT	1.4 (+2.0)	1.73 (+0.20)	1.78 (+0.14)	1.67 (+0.23)
ΔB_z/mT	1.9 (+1.2)	1.66 (+0.46)	1.71 (+0.16)	1.42 (+0.55)

[a]Chloronaphthalene/toluene 1:3, 9.2−34.5 GHz. [b]The best fit result was obtained for these *g* values. The rhombicity of **4** is 6 times smaller than the rhombicity of the aryl imido complexes and remains unresolved at Q-band.

symmetric complexes **5** and **7** compared to the C_{4v}-symmetric octahedral complexes **4** and **6**.[48] This may be caused by overlap of one of the Mo−N_{imido}-π-orbitals (Mo(d_{xz})-N(p_x) or Mo(d_{yz})-N(p_y)) and the aromatic system of the mesityl group. This might be verified in future investigations by theoretical calculations.

Crystal Structure of 5. Suitable crystals of **5** for X-ray diffraction were obtained from a saturated CH_2Cl_2 solution at 4 °C. **5** crystallizes in the cubic space group $Im\bar{3}$. Three disordered solvent molecules per phthalocyanine are present in the crystal structure. Selected crystallographic data are summarized in Table 2.

Table 2. Selected Crystallographic Data for 5

formula	$C_{77}H_{91}Cl_9MoN_9$
formula weight	1557.58
crystal system	cubic
space group	$Im\bar{3}$
a, *b*, *c*, Å	29.5000(4)
α, *β*, *γ*, deg	90
V, Å^3	25672(6)
Z	12
D_{calcd}, g/cm^3	1.209
μ, cm^{-1}	0.478
F(000)	9732
crystal size, mm^3	0.23 × 0.19 × 0.11
reflns collected	11783
independent reflns	4773
R_{int}	0.0809
R indices [$I > 2\sigma(I)$][a]	R_1 = 0.0561, wR_2 = 0.1226
R indices (all data)	R_1 = 0.1448, wR_2 = 0.1386

[a]$R_1 = [\sum||F_o| - |F_c||/\sum|F_o|]$; $wR_2 = [\sum[w(F_o^2 - F_c^2)^2]/\sum(wF_o^4)]^{1/2}$.

The molecular structure of **5** is displayed in Figure 6. Because of the symmetry of the molecule, only one-quarter of the complex is present in the asymmetric unit. Therefore, the orientation of the axial mesityl substituent is disordered with equal occupation. The coordination geometry around the central molybdenum atom is distorted octahedral and compares well with the structure of [PcMo(NtBu)Cl].[17] Selected bond lengths and angles are summarized in Table 3. The imido and chlorido ligands occupy the axial positions with a linear N4−Mo1−Cl1 alignment (180°). The equatorial positions are occupied by the isoindoline N atoms. The metal is located

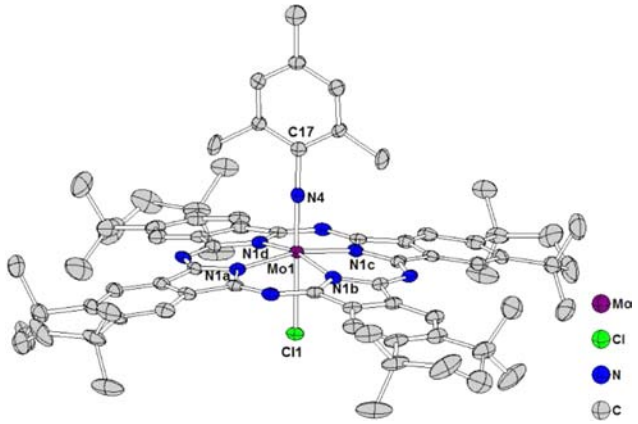

Figure 6. Molecular structure of **5**. H atoms and disorder of the mesityl group are omitted for clarity. Symmetry operation used to generate equivalent atoms: a: −*x*,*y*,*z*; b: −*x*,−*y*+1,*z*; c: *x*,−*y*+1,*z*; d: −*x*,*y*,−*z*.

Table 3. Selected Bond Lengths (Å) and Angles (deg) in 5

Mo1−N1	2.054(2)	Cl1−Mo1−N4	180
Mo1−N4	1.720(5)	N1−Mo1−N1a	89.4(2)
N4−C17	1.398(8)	N1−Mo1−N1b	165.6(2)
Mo1−Cl1	2.503(2)	N4−C17−$Mes_{Centroid}$	171.1
N1−Mo1−N4	97.2(1)	$dMo_{out\ of\ plane}$	0.257
Mo1−N4−C17	180		

0.257 Å above the plane defined by the four isoindoline N atoms. The displacement is thus smaller than in [PcMo(NtBu)Cl] ($d_{out\ of\ plane}$ = 0.305 Å).[17] The aromatic system deviates slightly from planarity, adapting a saucer conformation. No significant differences between the inner core Pc systems in **5** and [PcMo(NtBu)Cl] can be observed.

The most striking differences between alkyl substituted [PcMo(NtBu)Cl] and aryl substituted **5** are the different Mo−Cl and Mo−N_{imido} distances. The molybdenum imido bond interaction in **5** (Mo1−N4 = 1.720(5) Å) is longer than in [PcMo(NtBu)Cl] (1.704(7) Å). In contrast to this, the Mo1−Cl1 distance in **5** (2.503(2) Å) is shorter than in [PcMo(NtBu)Cl] (2.600(2) Å). These differences between the alkyl and aryl imido complexes can be explained by the thermodynamic *trans*-effect due to the *trans*-alignment of the π-donor ligands Cl and NR. The imido nitrogen atom in [PcMo(NtBu)Cl] is a better π donor, it is more electron rich

dx.doi.org/10.1021/ic3026914 | Inorg. Chem. 2013, 52, 4451−4457

because of the +I effect of the *t*Bu-group. As a consequence, the Mo−N bond is rather short, while the *trans* Mo−Cl bond is elongated. The mesityl group exhibits a −I effect leading to a less electron rich imido nitrogen atom. Consequently, the Mo−N bond is longer, while the Mo−Cl bond is shorter. This structural difference between **5** and [PcMo(N*t*Bu)Cl] is in good agreement with the observed differences in the EPR and UV−vis spectra of alkyl and aryl imido complexes **4**−**7**.

The semiconducting properties of phthalocyanines and related compounds depend largely on the crystal packing and the intermolecular interaction of the aromatic systems. The molecular arrangement of the **5** molecules in the unit cell is displayed in Figure 7. The aromatic systems are aligned as

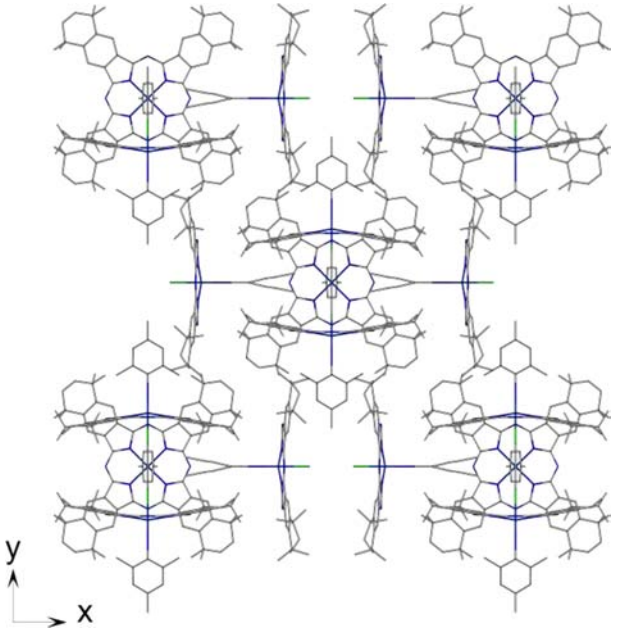

Figure 7. Molecular arrangement of **5**. H atoms and four molecules of CH_2Cl_2 per **5** are omitted for clarity. Both orientations of the disordered mesityl group are occupied equally.

dimers, with the concave sides of two neighboring molecules facing each other. The dimers are tilted about 90° with respect to the neighboring dimers, leading to a cubic structure. This arrangement resembles the crystal structure of [Pc$^{\#}$TiCl$_2$],[21] where a cubic arrangement of Pc$^{\#}$-dimers is also present. In contrast to this, a layered arrangement of the aromatic systems was found for the unsubstituted Pc complex [PcMo(N*t*Bu)-Cl].[17]

CONCLUSION

In this work we described the synthesis of soluble, axially functionalized molybdenum(V) phthalocyanines and pyrazinoporphyrazines **4**−**7**. Ppz$^{\#}$ compounds **6**−**7** are the first examples of molybdenum pyrazinoporphyrazines described in literature. The properties of **4**−**7** were analyzed by UV−vis and EPR spectroscopy. The Q-band absorption maximum depends on the nature of the macrocyclic complexes. A hypsochromic shift of 76−80 nm is observed upon exchange of the electron rich Pc$^{\#}$ ligand for the electron deficient Ppz$^{\#}$ ligand. However, the dependence of the Q-band absorption maximum on the nature of the axial ligand was somewhat unexpected. EPR spectroscopic analyses revealed the different symmetries of the alkyl and aryl imido complexes. N*t*Bu-substituted complexes **4** and **6** were found to be C_{4v} symmetric, while the symmetry in NMes-substituted complexes **5** and **7** is lowered to C_{2v}. This could also be confirmed by the crystal structure of [Pc$^{\#}$Mo(NMes)Cl] **5**. These results show how the combination of UV−vis and EPR spectroscopy can be utilized to understand the properties of axially functionalized, paramagnetic phthalocyanine and pyrazinoporphyrazine complexes. Furthermore, we introduced a new highly symmetric, isomerically pure octaalkyl pyrazinoporphyrazine ligand Ppz$^{\#}$. It is compact and more rigid compared to octa-*n*-alkyl derivatives of similar molar mass. Therefore it tends to form crystalline phases, while still being soluble and only weakly aggregating. This is the precondition for its use in many optoelectronic applications such as in photosensitizers for singlet oxygen formation or in photoanodes of organic solar cells. Further development of Ppz$^{\#}$ coordination and photo chemistry will be explored in due time.

ASSOCIATED CONTENT

Supporting Information

CIF data for **5**. This material is available free of charge via the Internet at http://pubs.acs.org.

AUTHOR INFORMATION

Corresponding Author

*E-mail: jsu@staff.uni-marburg.de. Fax: +49 (0)6421 28-25711. Tel: +49 (0)6421 28-256.

Notes

The authors declare no competing financial interest.

REFERENCES

(1) Wöhrle, D.; Schnurpfeil, G.; Makarov, S.; Suvora, O. *Chem. unserer Zeit* **2012**, *46*, 12−24.

(2) (a) *Phthalocyanines, Properties and Applications*; Leznoff, C. C., Lever, A. B. P., Eds.; Wiley-VCH: New York, 1989; (b) *Phthalocyanine Materials: Synthesis, Structure, and Function*, McKeown, N. B., Ed.; Cambridge University Press: New York, 1998; (c) *Functional Phthalocyanine Molecular Materials*; Jiang, J., Ed.; Springer: Berlin, Germany, 2010.

(3) Engel, M. K. Phthalocyanines: Structural Characterization. In *The Porphyrin Handbook*; Kadish, K. M., Smith, K. M., Guilard, R., Eds.; Academic Press: San Diego, CA, 2003; Vol. *20*, pp 1−88.

(4) Linstead, R. P.; Lowe, A. R. *J. Chem. Soc.* **1934**, 1016−1017.

(5) (a) Hanack, M.; Heckmann, H.; Polley, R., 2. Phthalocyanines and Related Compounds. In *Houben-Weyl, Methods of Organic Chemistry, F: Aromatic and Heteroaromatic Large Rings*; Thieme: Stuttgart, Germany, 1997, Vol. *4*, pp 717−842; (b) Efimova, S. V.; Koifman, O. I.; Bykova, V. V.; Lukyanov, Yu.; Sotsky, V. V.; Usol'tseva, N. V. *Mol. Cryst. Liq. Cryst.* **2012**, *553*, 66−71. (c) Belozerova, Yu. I.; Efimova, S. V.; Korzhenevskii, A. B.; Koifman, O. I. *Russ. J. Gen. Chem.* **2009**, *79*, 2678−2684.

(6) Zaumseil, J.; Sirringhaus, H. *Chem. Rev.* **2007**, *107*, 1296−1323.

(7) Bruder, I.; Ojala, A.; Lennartz, C.; Sundarraj, S.; Schöneboom, J.; Sens, R.; Hwang, J.; Erk, P.; Weis, J. *Sol. Energy Mater. Sol. Cells* **2010**, *94*, 310−316.

(8) Bruder, I.; Schöneboom, J.; Dinnebier, R.; Ojala, A.; Schäfer, S.; Sens, R.; Erk, P.; Weis, J. *Org. Electron.* **2010**, *11*, 377−387.

(9) Palomares, E.; Martinez-Diaz, M. V.; Haque, S. A.; Torres, T.; Durrant, J. R. *Chem. Commun.* **2004**, 2112−2113.

(10) Walter, M. G.; Rudine, A. B.; Wamser, C. C. *J. Porphyrins Phthalocyanines* **2010**, *14*, 759−792.

(11) Imahori, H.; Umeyama, T.; Ito, S. *Acc. Chem. Res.* **2009**, *42*, 1809−1818.

(12) López-Duarte, I.; Wang, M.; Humphry-Baker, R.; Ince, M.; Martinez-Diaz, M. V.; Nazeeruddin, M. K.; Torres, T.; Grätzel, M. *Angew. Chem., Int. Ed.* **2012**, *51*, 1895−1898.

(13) Reddy, P. Y.; Giribabu, L.; Lyness, C.; Snaith, H. J.; Vijaykumar, C.; Chandrasekharam, M.; Lakshmikantam, M.; Yum, J.-H.; Kalyanasundaram, K.; Grätzel, M.; Nazeeruddin, M. K. *Angew. Chem., Int. Ed.* **2007**, *46*, 373−376.
(14) (a) de la Torre, G.; Vazquez, P.; Agullo-Lopez, F.; Torres, T. *J. Mater. Chem.* **1998**, *8*, 1671−1683. (b) Flaherty, S. M. O.; Hold, S. V.; Cook, M. J.; Torres, T.; Hanack, M.; Blau, W. J. *Adv. Mater.* **2003**, *15*, 19−32. (c) de la Torre, G.; Vazquez, P.; Agullo-Lopez, F.; Torres, T. *Chem. Rev.* **2004**, *104*, 3723−3750. (d) Hanack, M.; Schneider, T.; Barthel, M.; Shirk, J. S.; Flom, S. R.; Pong, R. G. S. *Coord. Chem. Rev.* **2001**, *219*, 235−258.
(15) Darwish, W.; Harms, K.; Sundermeyer, J. *Acta Crystallogr.* **2005**, *E61*, m1280−m1282.
(16) Darwish, W.; Schlecht, S.; Schaper, A.; Fröba, M.; Harms, K.; Massa, W.; Sundermeyer, J. *Z. Anorg. Allg. Chem.* **2009**, *635*, 1215−1224.
(17) Darwish, W.; Seikel, E.; Harms, K.; Burghaus, O.; Sundermeyer, J. *Dalton Trans.* **2011**, *40*, 1183−1188.
(18) Darwish, W.; Seikel, E.; Käsmarker, R.; Harms, K.; Sundermeyer, J. *Dalton Trans.* **2011**, *40*, 1787−1794.
(19) Frick, K.; Verma, S.; Sundermeyer, J.; Hanack, M. *Eur. J. Inorg. Chem.* **2000**, *13*, 1025−1030.
(20) Seikel, E.; Grau, M.; Käsmarker, R.; Oelkers, B.; Sundermeyer, J. *Inorg. Chim. Acta* **2011**, *374*, 119−126.
(21) Seikel, E.; Oelkers, B.; Sundermeyer, J. *Inorg. Chem.* **2012**, *51*, 2709−2717.
(22) Mikhalenko, S. A.; Solov'eva, L. I.; Luk'yanets, E. A. *J. Gen. Chem. USSR* **1988**, *58*, 2618−2619.
(23) Dieng, M.; Contamin, O.; Savy, M. *Electrochim. Acta* **1988**, *33*, 121−126.
(24) Sheldon, R. A. *Recl. Trav. Chim. Pays-Bas* **1973**, *92*, 253−266.
(25) Savy, M.; Coowar, F.; Riga, J.; Verbist, J. J.; Bronoël, G.; Besse, S. *J. Appl. Electrochem.* **1990**, *20*, 260−268.
(26) Arzoumanidis, G. G.; O'Connell, J. J. *J. Phys. Chem.* **1969**, *73*, 3508−3510.
(27) Edmondson, S. J.; Mitchell, P. C. H. *Polyhedron* **1986**, *5*, 315−317.
(28) Nyokong, T. *Inorg. Chim. Acta* **1989**, *160*, 235−239.
(29) Verma, S.; Hanack, M. *Z. Anorg. Allg. Chem.* **2003**, *629*, 880−892.
(30) Gorsch, M.; Homborg, H. *Z. Anorg. Allg. Chem.* **1998**, *624*, 634−641.
(31) Gal'pern, E. G.; Luk'yanets, E. A.; Gal'pern, M. G. *Russ. Chem. Bull.* **1973**, *22*, 1925−1929.
(32) Zimcik, P.; Novakova, V.; Kopecky, K.; Miletin, M.; Kobak, R. Z. U.; Svandrlikova, E.; Váchocá, L.; Lang, K. *Inorg. Chem.* **2012**, *51*, 4215−4223.
(33) Further synthetic and spectroscopic investigations of the free ligand $Ppz^{\#}H_2$ and the respective 3d and main group metal complexes will be discussed in a separate publication.
(34) Coffman, D. D.; Jenner, E. L.; Lipscomb, R. D. *J. Am. Chem. Soc.* **1958**, *80*, 2864−2872.
(35) Jones, P.; Villeneuve, G. B.; Fei, C.; DeMarte, J.; Haggarty, A. J.; Nwe, K. T.; Martin, D. A.; Lebuis, A.-M.; Finkelstein, J. M.; Gour-Salin, B. J.; Chan, T. H.; Leyland-Jones, B. R. *J. Med. Chem.* **1998**, *41*, 3062−3077.
(36) Dyer, P. W.; Gibson, V. C.; Howard, J. A. K.; Whittle, B.; Wilson, C. *Polyhedron* **1995**, *14*, 103−111.
(37) Radius, U.; Sundermeyer, J.; Pritzkow, H. *Chem. Ber.* **1994**, *127*, 1827−1835.
(38) Rieger, P. H. *Electron Spin Resonance - Analysis and Interpretation*; RSC Publishing: Cambridge, U.K., 2007.
(39) Hagen, W. R. *Biomolecular EPR Spectroscopy*; CRC Press: Boca Raton, FL, 2009.
(40) *Stoe X-AREA and X-RED*; Stoe & Cie GmbH: Darmstadt, Germany, 2001.
(41) Farrugia, J. L. *J. Appl. Crystallogr.* **1999**, *32*, 837−838.
(42) Burla, M. C.; Caliandro, R.; Camalli, M.; Carrozzini, B.; Cascarano, G. L.; De Caro, L.; Giacovazzo, C.; Polidori, G.; Spagna, R. *J. Appl. Crystallogr.* **2005**, *38*, 381−388.
(43) Sheldrick, G. M. *Acta Crystallogr., Sect. A* **2008**, *64*, 112−122.
(44) Brandenburg, K. *Diamond 3.2*; Crystal Impact GbR: Bonn, Germany, 2011.
(45) Barthel, M.; Hanack, M. *J. Porphyrins Phthalocyanines* **2000**, *4*, 635.
(46) Kim, J. C.; Rees, W. S.; Goedken, V. L. *Inorg. Chem.* **1995**, *34*, 2483−2486.
(47) Basu, P. *J. Chem. Educ.* **2001**, *78*, 666−669.
(48) Serwicka, E. *J. Solid State Chem.* **1984**, *51*, 300−306.

dx.doi.org/10.1021/ic3026914 | *Inorg. Chem.* 2013, 52, 4451−4457